This is a repository copy of *Performance of a hybrid powertrain employing a magnetic power split device*.

White Rose Research Online URL for this paper:
http://eprints.whiterose.ac.uk/148145/

Version: Accepted Version

Proceedings Paper:
Hoang, K. orcid.org/0000-0001-7463-9681, Atallah, K., Odavic, M. et al. (2 more authors) (2019) Performance of a hybrid powertrain employing a magnetic power split device. In: 2019 IEEE Energy Conversion Congress and Exposition (ECCE). 2019 IEEE Energy Conversion Congress and Exposition (ECCE), 29 Sep - 03 Oct 2019, Baltimore, MD, USA. IEEE . ISBN 9781728103969

https://doi.org/10.1109/ECCE.2019.8913307

© 2019 IEEE. Personal use of this material is permitted. Permission from IEEE must be obtained for all other users, including reprinting/ republishing this material for advertising or promotional purposes, creating new collective works for resale or redistribution to servers or lists, or reuse of any copyrighted components of this work in other works. Reproduced in accordance with the publisher's self-archiving policy.

Reuse
Items deposited in White Rose Research Online are protected by copyright, with all rights reserved unless indicated otherwise. They may be downloaded and/or printed for private study, or other acts as permitted by national copyright laws. The publisher or other rights holders may allow further reproduction and re-use of the full text version. This is indicated by the licence information on the White Rose Research Online record for the item.

Takedown
If you consider content in White Rose Research Online to be in breach of UK law, please notify us by emailing eprints@whiterose.ac.uk including the URL of the record and the reason for the withdrawal request.

eprints@whiterose.ac.uk
https://eprints.whiterose.ac.uk/

Performance of a Hybrid Powertrain Employing a Magnetic Power Split Device

Khoa D Hoang, Kais Atallah, and Milijana Odavic
Dept. of Electronic and Electrical Engineering
The University of Sheffield
Sheffield, United Kingdom
https://orcid.org/0000-0001-7463-9681
https://orcid.org/0000-0002-8008-8457
https://orcid.org/0000-0002-2104-8893

Jeff Birchall and Stuart Calverley
Magnomatics Limited
Park House, Bernard Road
Sheffield, S2 5BG, United Kingdom
j.birchall@magnomatics.com
s.calverley@magnomatics.com

***Abstract*—In this paper, performance of a magnetic power split device (MAGSPLIT) employed for hybrid powertrain is evaluated via measurements and presented for both component level (stand-alone device) and system level (MAGSPLIT-based hybrid powertrain). It is shown that a MAGSLPIT-based hybrid powertrain can provide similar functionalities as conventional mechanical power split hybrid powertrain but with a number of advantages including inherent torsional vibration attenuation, simplification of mechanical arrangement, and potentially improved efficiency through the elimination of some mechanical losses. It is demonstrated that for a MAGSPLIT-based hybrid powertrain, torque and speed of its internal combustion engine (ICE) can be independently controlled. This may lead to maximum ICE efficiency achievement by controlling ICE speed and torque following its maximum fuel efficiency line.**

Keywords— hybrid powertrain, internal combustion engine, magnetic power split device, torque oscillation attenuation.

I. Introduction

Recently, due to its good capabilities for reducing vehicle emissions and improving efficiency, hybrid powertrains are attracting a lot of interest [1]. Among the mature hybrid powertrain concepts, the well-known Hybrid Synergy Drive (HSD) powertrain [2]-[3] developed by Toyota can provide a lot of advantages, Fig. 1(a). As can be seen, the HSD concept employs an internal combustion engine (ICE), two electrical machines (MG1 mainly working in generating mode and MG2 mainly working in motoring mode) and a mechanical power-split device (PSD) acting as a continuously variable transmission (CVT). By way of example, by independently controlling the ICE following its maximum operating efficiency curve, the PSD can be employed to distribute ICE power to the final drive and the MG2 via the MG1 in charge neutral mode; allow the MG2 to boost the final drive power using battery power when high power demand required; deliver ICE power via MG1 to charge the battery pack in charge sustaining mode; and let only the MG2 to power the final drive in charge depleting (EV) mode.

In comparison with the HSD concept, the magnetic power split device (MAGSPLIT or MS) [4] based on magnetic gearing concept [5] in Fig. 1(b) can provide similar combined functionalities of both PSD and MG1 but with a number of advantages such as inherent torsional vibration attenuation since power and torque is transmitted from the ICE to the final drive (FD) via magnetic coupling, simplification of mechanical arrangement resulting in potentially improved powertrain reliability and efficiency. However, MAGSPLIT concept is still at its early development phase, with the first paper describing the concept can be tracked back to 2012 [6] and modified MAGSPLIT concepts were recently presented in [7] and [8], respectively. In addition, studies of its operation are still relatively limited [9]-[10].

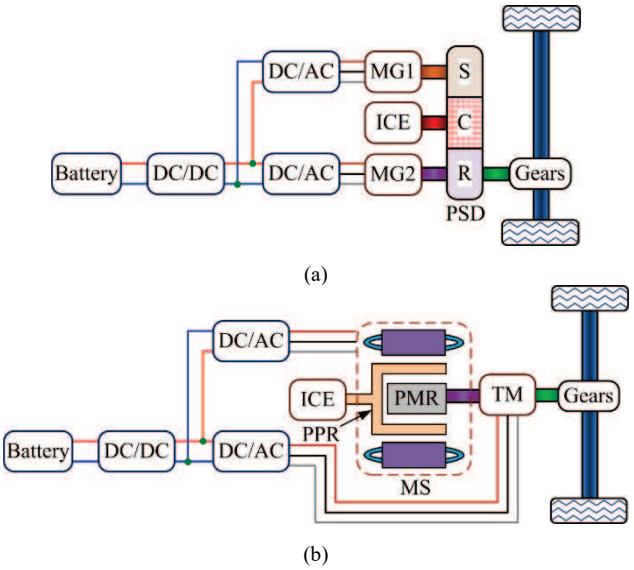

Fig. 1. CVT hybrid powertrain. (a) HSD-based concept [1]-[3]. (b) MAGSPLIT-based concept [5] and [10].

The paper presents a performance evaluation of MAGSPLIT at component level (stand-alone device) and system level (hybrid powertrain). It is shown that a MAGSPLIT can maintain power and torque transmission in a similar fashion as combined PSD and MG1 of the well-known HSD concept, Fig. 1(a), without requirement for a rigid mechanical connection. It is also shown that when integrated into a hybrid powertrain (system level test), despite the significant ripples in torque produced by the ICE, negligible oscillations are transmitted to the final drive. In addition, it is also presented that for a MAGSPLIT-based hybrid powertrain with ICE is controlled to deliver demanded torque, ICE speed can be independently controlled by the MAGSPLIT. Therefore, by controlling ICE speed and torque following its maximum fuel efficiency line, maximum ICE efficiency for MAGSPLIT-based hybrid powertrain may be obtained.

II. MAGSPLIT Modelling

As shown in Fig. 2(a), a MAGSPLIT (MS) includes a stator winding and two rotors: an inner PM rotor (PMR) and an outer pole piece rotor (PPR) [4]. Based on magnetic gearing concepts [5], appropriate number of poles for rotating magnetic fields generated by the stator windings, the PMR, and the number of pole-pieces on the PPR are determined to enable and maximize the magnetic coupling between the stator winding and the two rotors [5]. The tested MAGSPLIT

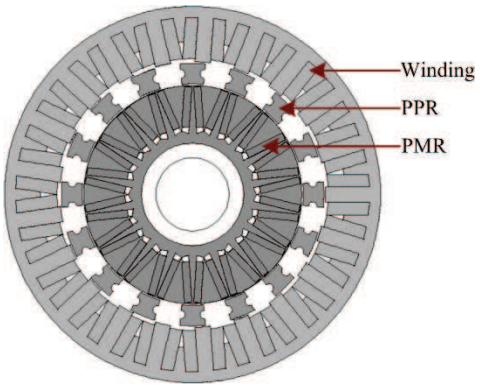

(a)

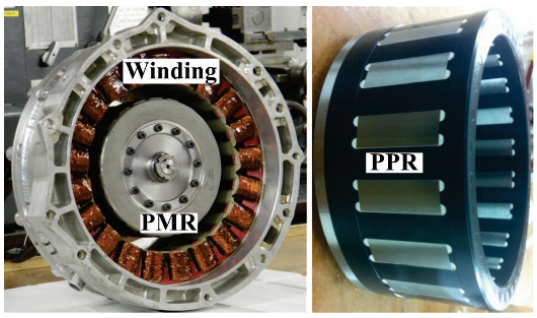

(b)

Fig. 2. MAGSPLIT specification. (a) Structure. (b) Tested MAGSPLIT [10].

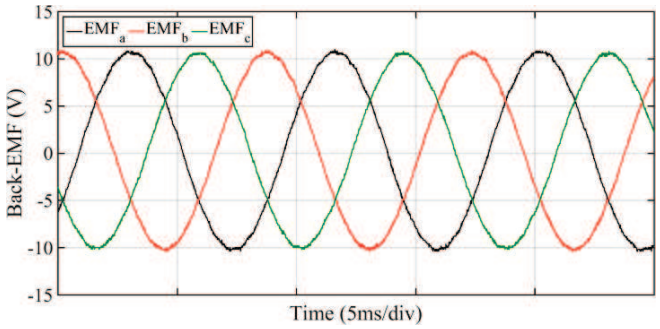

(a)

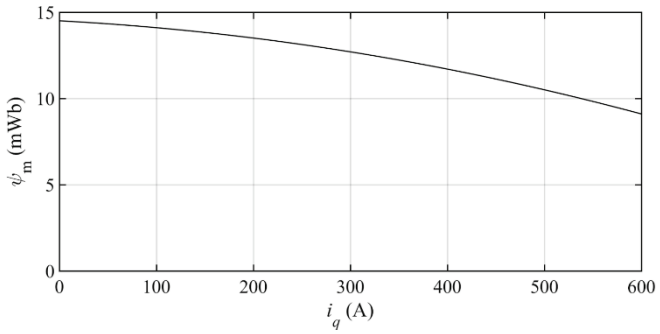

(b)

Fig. 3. Electrical specifications of tested MAGSPLIT. (a) Back-EMF with PPR speed is as zero, PMR speed is as 1000rpm. (b). PM flux linkage as a function of q-axis current.

is illustrated in Fig. 2(b) and its parameters are presented in Table I.

A. Mechanical Modelling

In [4], [6], and [10], MAGSPLIT operation has been introduced, and the relationships between speed and torque of

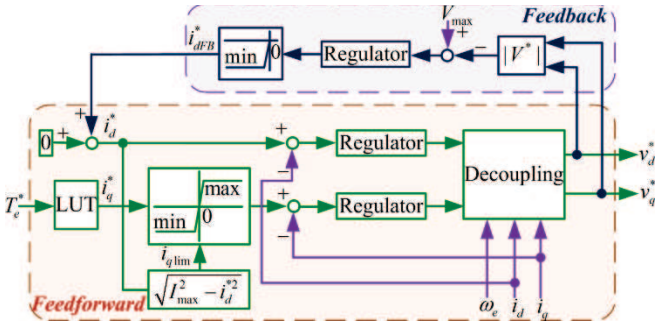

(a)

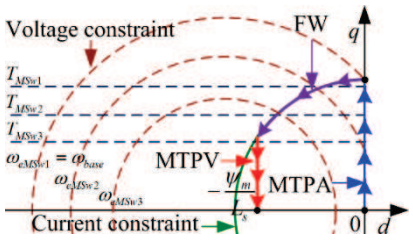

(b)

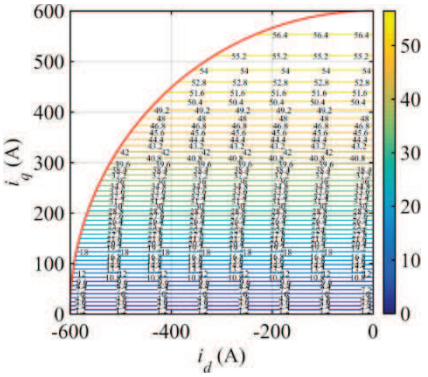

(c)

Fig. 4. MAGSPLIT control development. (a) Control technique. (b) Operating regions. (c) Torque map.

TABLE I

SPECIFICATIONS OF TESTED MAGSPLIT

Rated torque (Nm) at PPR	160
Rated current (A)	600
Resistance (mΩ)	5.7
Phase inductance (μH)	105.6
PM flux linkage (mWb)	14.5
Maximum speed (rpm)	6000
DC-link voltage (V)	600
Number of PPR	16
Number of PMR pole pair	9
Number of MSw pole pair	7

the PPR, the PMR, and the MAGSPLIT stator winding (MSw) is as follows:

$$\omega_{PPR} n_{PPR} = \omega_{PMR} n_{PMR} + \omega_{MSw} n_{MSw} \tag{1}$$

$$T_{MSw}(n_{PPR} / n_{MSw}) = T_{PMR}(n_{PPR} / n_{PMR}) = -T_{PPR} \tag{2}$$

$$J_{\Sigma PPR} \frac{d\omega_{PPR}}{dt} = T_{PPR} + T_{PPR}^{ext} \tag{3.a}$$

$$J_{\Sigma PMR} \frac{d\omega_{PMR}}{dt} = T_{PMR} + T_{PMR}^{ext} \tag{3.b}$$

where ω_{PPR}, ω_{PMR}, and ω_{MSw} are the rotational speeds of PPR, PMR, and the magnetic field generated by the stator winding, respectively; T_{PPR}, T_{PMR}, and T_{MSw} are the torque of PPR, PMR, and stator winding, respectively; n_{PPR}, n_{PMR}, and n_{MSw} are the number of pole-pieces on PPR, the number of pole pairs on PMR, and the number of pole pairs of rotating stator magnetic field, respectively. Furthermore, $J_{\Sigma PPR}$ and $J_{\Sigma PMR}$ are the total inertias rigidly connected to PPR and PMR, respectively; the superscript "*ext*" denotes the external torque applied to the relevant rotor.

It is noted that when operating speeds of the PPR and PMR are the same, by considering (1), a similar rotational speed for magnetic field generated by the stator winding is also required to maintain the magnetic coupling principal. This theory will be validated under component level test of the MAGSPLIT in the next section.

B. Electrical Modelling

Due to large equivalent airgap length, Fig. 2, the MAGSPLT stator winding coupling with PPR and PMR can be modelled as a surface-mounted synchronous PM (SPM) machine [10]:

$$v_d = R_s i_d + \frac{d\psi_d}{dt} - \omega_{eMSw}\psi_q \tag{4.a}$$

$$v_q = R_s i_q + \frac{d\psi_q}{dt} + \omega_{eMSw}\psi_d \tag{4.b}$$

$$\psi_d = L_s i_d + \psi_m \tag{5.a}$$

$$\psi_q = L_s i_q \tag{5.b}$$

$$T_{MSw} = (3/2) n_{MSw} \psi_m i_q \tag{6}$$

where $v_{d,q}$, $i_{d,q}$, $\psi_{d,q}$, are the transformed (dq) voltages, currents, and stator flux-linkages, respectively; L_s is the stator synchronous inductance; ω_{eMSw} is the stator electrical speed; R_s is the stator winding resistance; ψ_m is the PM flux linkage associated with the space harmonic coupled to the stator winding.

The tested MAGSPLIT back-EMF (electromotive force) with inherently sinusoidal waveform is depicted in Fig. 3(a) and its permanent magnet (PM) flux linkage considering saturation is illustrated in Fig. 3(b). MAGSPLIT electrical parameters are presented in Table I. For controlling the MAGSPLIT, SPM machine control methodology is selected, Fig. 4(a), and relevant operating regions is shown in Fig. 4(b). The tested MAGSPLIT torque map as a function of dq-axis currents is introduced in Fig. 4(c).

III. MAGSPLIT Performance as Stand-Alone Device

A. Test-rig

The purpose of this test is to evaluate MAGSPLIT performance associated with its magnetic coupling relationship shown in (1) to (3). A test-rig has been developed as shown in Fig. 5(a) and its schematic layout is depicted in Fig. 5(b) where two induction machine drives in speed control mode are connected to the two MAGSPLIT rotors. The drive machine (DM) connected to the PPR represents the input power while the load machine (LM) linked to the PMR simulates the output load. The MAGSPLIT winding magnetic field (MSw) is controlled by another industrial drive (MS drive) under torque control mode using control method presented in Fig. 4. Measurement equipment such as torque transducer (TT) and data acquisition (DAQ) is employed to capture torque (Tq), speed (Spd), current, voltage, power (Pwr), and efficiency.

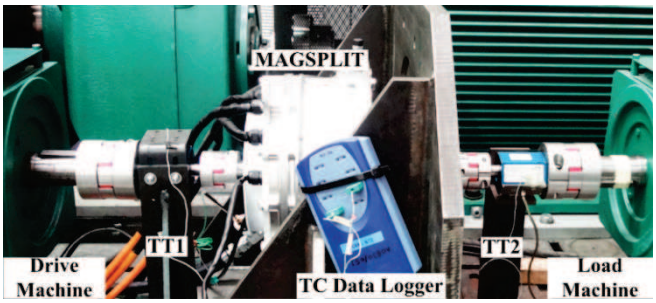

(a)

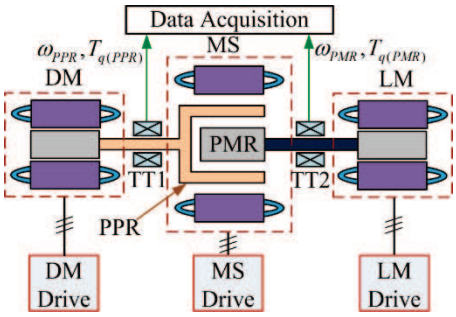

(b)

Fig. 5. MAGSPLIT test-rig at component level. (a) Test-rig arrangement. (b) Test-rig illustration.

B. Test Results

To validate MAGSPLIT magnetic coupling relationship given by (1) to (3), a ramp speed (Ramp Spd) acceleration from standstill to 500 rpm is demanded for both DM and LM. From Fig. 6(a), it can be seen that the speeds of MSw and the two rotors are similar to satisfy equation (1) as aforementioned. At 10s, a ramp torque (Ramp Tq) from 0 to 86% of its PPR rated value (155Nm) is applied to MSw. Figs. 6(b) and 6(c) show the resulting torques and relevant transmission torque ratios from PPR to PMR (16/9) and from PPR to MSw (16/7).

In addition, the power contribution of tested MAGSPLIT is introduced in Fig. 6(d) where it can be seen that under this particular condition the power is input through the PPR and output through the PMR and the MS stator.

Furthermore, efficiency during ramp torque operation in Fig. 6 is presented in Fig. 7(a) where a maximum efficiency of 95% can be achieved. Figs. 7(b) and 7(c) respectively show measured efficiencies of the MAGSPLIT at half and full load under different PPR and PMR operating speed with an efficiency in excess of 97% can be obtained.

IV. MAGSPLIT Performance in a Hybrid Powertrain

A. Test-rig

For MAGSPLIT performance evaluation in a powertrain, a MAGSPLIT-based hybrid powertrain test-rig is developed as shown in Figs. 8(a) and 8(b) including an ICE connected in-line with a MAGSPLIT and a traction machine-TM. A load machine (LM) acting as the vehicle tractive load is connected to the test-rig via a belt drive (BR). Three torque transducers

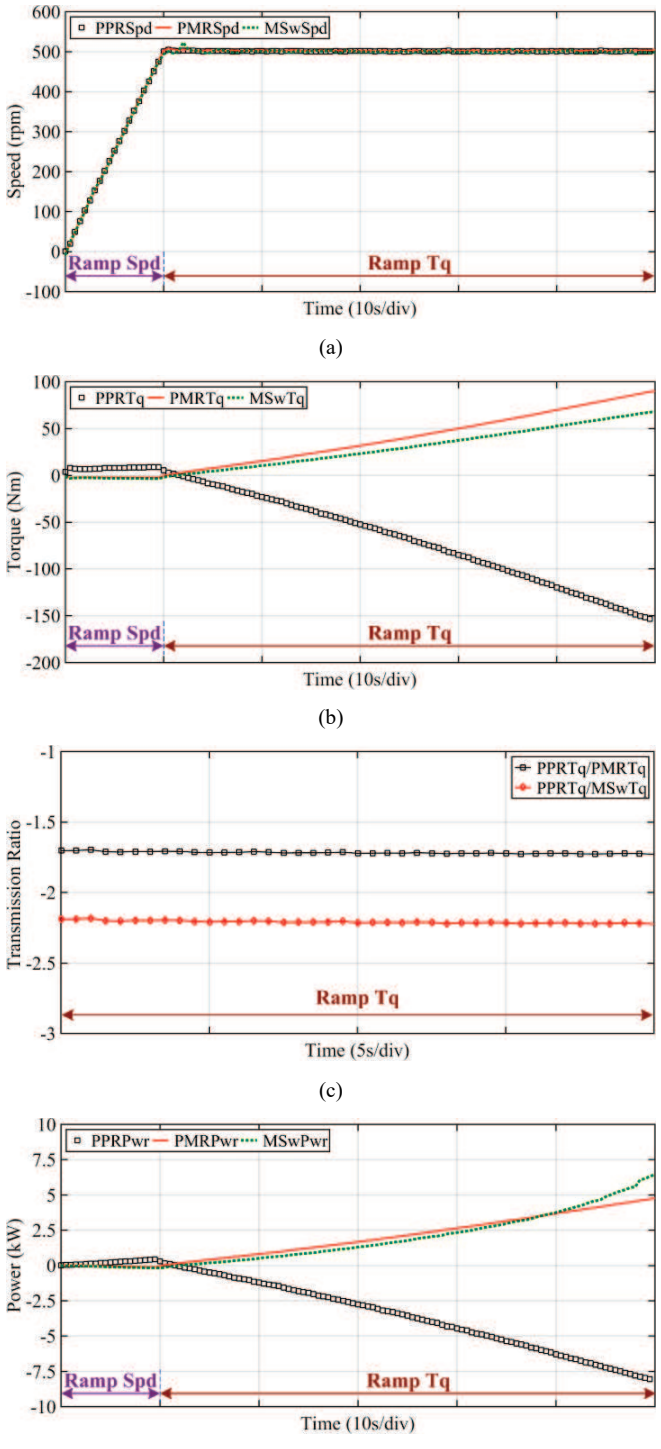

Fig. 6. MAGSPLIT performance evaluation at component level. (a) Speed response. (b) Torque response. (c) Torque transmission ratio. (d) Power response.

(TT) are installed to capture PPR torque (TT1), PMR torque (TT2), and final drive (FD) torque (TT3). Two resolvers (RS) are utilized to provide PPR (RS1) and PMR (RS2) position/speed information which are essential for MAGSPLIT operation. A MotoHawk ECM-5554-112 is employed as a hybrid traction control unit (HTCU) communicating with other device controllers via CAN bus. It is noted that in this test, ICE and TM are operated under torque control mode while ICE speed is controlled by the MAGSPLIT. The purpose of this test is to demonstrate how a

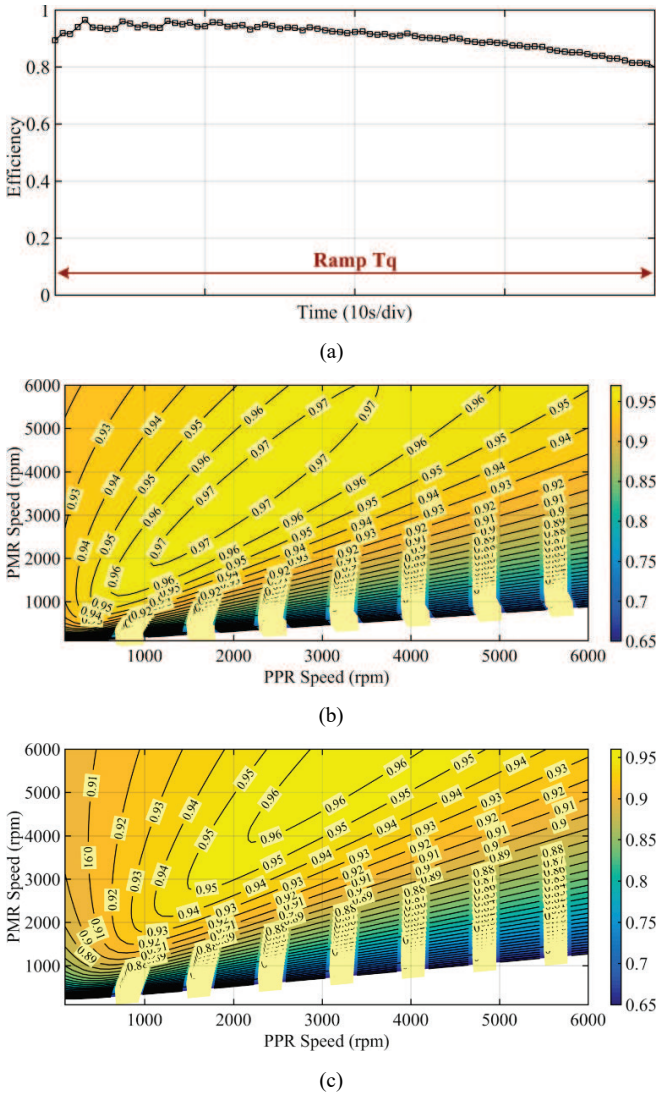

Fig. 7. MAGSPLIT efficiency. (a) Efficiency during ramp torque operation in Fig. 6. (b) Half rated torque under different PMR and PPR speed. (c) Full rated torque under different PMR and PPR speed.

MAGSPLIT can be integrated to a hybrid powertrain to provide similar combined functionalities as a PSD and MG1 in a HSD-based hybrid powertrain, Fig. 1(a) but with simplification of mechanical arrangement and inherent torque oscillation attenuation characteristic.

B. Test Results

Measurements of dynamic torque response from the hybrid powertrain test-rig under dynamic torque evaluation are presented in Fig. 9. For demonstration purpose, similar direction is selected for both PPR torque (ICE torque) and PMR torque. First, the ICE speed is accelerated from standstill to 1200rpm by the MAGSPLIT with powertrain torque demand (FDTq) is set to zero. Fig. 9(a) presents the dynamic torques with the ICE speed is controlled in the steady-state by the MAGSPLIT at 1200rpm. During t_1, t_2 and t_3, powertrain torque demand (FDTq) is set to zero with engine torque set as 10Nm for t_1, 20Nm for t_2, and 30Nm for t_3 resulting in relevant transmitted torques to the PMR. Thus, to maintain a zero powertrain torque demand at the final drive, the traction machine must act to balance the PMR torque. For t_4, t_5, and t_6, the powertrain torque demand is increased with 10Nm steps, respectively, while the engine torque is kept at 30Nm. Therefore, a constant output MAGSPLIT torque at the PMR

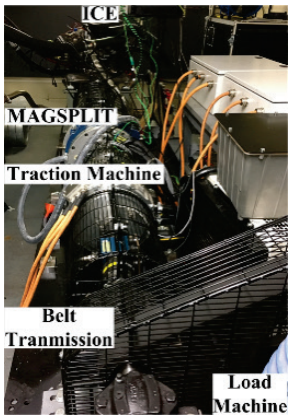

(a)

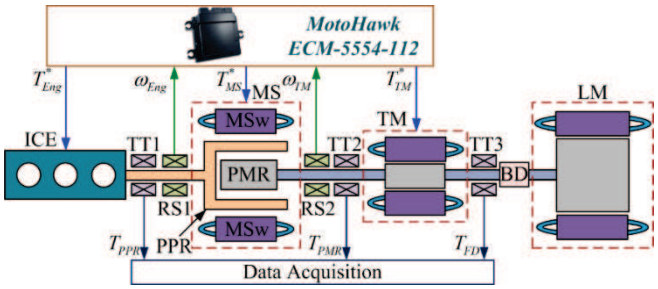

(b)

Fig. 8. MAGSPLIT test-rig at system level. (a) Test-rig arrangement. (b) Test-rig illustration.

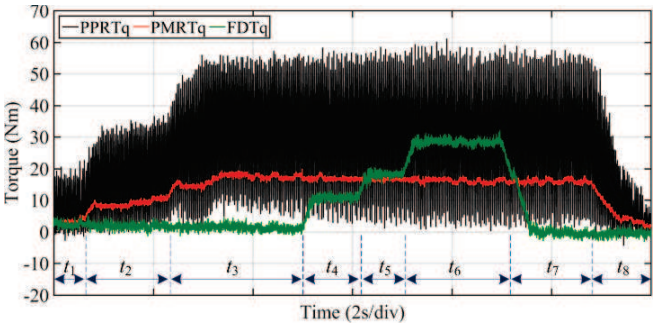

(a)

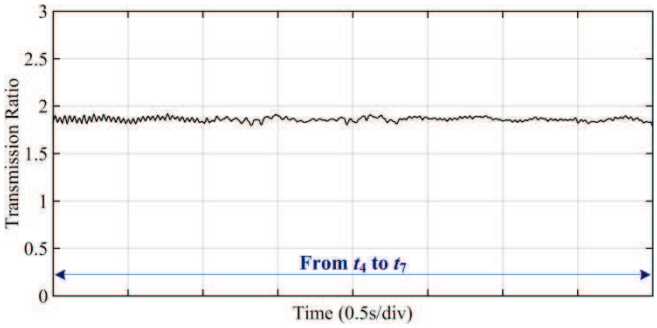

(b)

Fig. 9. MAGSPLIT performance evaluation at system level with MAGSPLIT-based hybrid powertrain. (a) Dynamic torque. (b) Relevant torque transmission ratio.

is maintained while the TM produces the difference to meet the required torque at the final drive. During t_7, the powertrain torque demand is reduced to zero while the engine torque is kept at 30Nm. For t_8, the engine torque is reduced to zero. As can be seen in Fig. 9(a), despite the very large ripple in the engine torque, the transmitted torque to the PMR exhibits very low ripple. This demonstrated an important advantage over the HSD-based powertrain in Fig. 1(a).

The relevant MAGSPLIT torque transmission ratio from the PPR to PMR (16/9) of dynamic torque response during t_4 to t_7 is shown in Fig. 9(b) which demonstrates the MAGSPLIT torque relation in (2). It is noted that since ICE is independently controlled by the MAGSPLIT while it is operated under torque control mode, maximum ICE efficiency for MAGSPLIT-based hybrid powertrain may be achieved by controlling ICE speed and torque following its maximum fuel efficiency line [10].

V. Conclusions

In this paper, component and system level performance evaluation of a magnetic power split device (MAGSPLIT) is presented. It is shown that a MAGSPLIT can maintain power and torque transmission via magnetic coupling in a similar fashion as combined PSD and MG1 of the well-known HSD concept without rigid mechanical connection requirement. Measurements show that an efficiency in excess of 97% can be obtained. On the other hand, torque oscillation attenuation characteristic of a MAGSPLIT-based hybrid powertrain is demonstrated with negligible oscillations are transmitted to the final drive despite the significant ripple in torque produced by the ICE and applied to the PPR. Furthermore, it is also demonstrated that for MAGSPLIT-based hybrid powertrain, the speed and torque of the ICE can be independently controlled to provide the required power at maximum efficiency.

References

[1] J. M. Miller, "Hybrid electric vehicle propulsion system architectures of the e-CVT type," *IEEE Trans. Power Electron.*, vol. 21, no. 3, pp. 756-767, May 2006.

[2] S. Sasaki, "Toyota 's newly developed hybrid powertrain," *Power Semiconductor Devices and ICs, ISPSD 98.*, Kyoto, 1998, pp. 17-22.

[3] K. D. Hoang and K. Atallah, "A rapid concept development technique for electric vehicle power trains," in *Proc. IEEE Int. Conf. Connected Vehicles and Export (ICCVE)* 2014, Vienna, Austria, Nov. 3-7, 2014, pp. 191-198.

[4] P. Chmelicek, S. D. Calverley, R. S. Dragan and K. Atallah, "Dual rotor magnetically geared power split device for hybrid electric vehicles," *IEEE Trans. Ind. Appl.*, vol. 55, no. 2, pp. 1484-1494, Mar.-Apr. 2019.

[5] K. Atallah, S. D. Calverley and D. Howe, "Design, analysis and realisation of a high-performance magnetic gear," in *IEE Proceedings - Electric Power Applications*, vol. 151, no. 2, pp. 135-143, 9 Mar. 2004.

[6] K. Atallah, J. Wang, S. D. Calverley, and S. Duggan, "Design and operation of a magnetic continuously variable transmission," *IEEE Trans. Ind. Appl.*, vol. 48, no. 4, pp. 1288 - 1295, Jul./Aug. 2012.

[7] M. Fukuoka, K. Nakamura, H. Kato and O. Ichinokura, "A novel flux-modulated type dual-axis motor for hybrid electric vehicles," *IEEE Trans. Magnetics*, vol. 50, no. 11, pp. 1-4, Nov. 2014.

[8] Morimoto, E, Niguchi, N, Hirata, K. Magnetic-geared motor with a continuously variable transmission gear ratio and its control method. *Electron Comm Jpn*. 2018; 101: 16– 26.

[9] L. Sun, M. Cheng, H. Wen, and L. Song, "Motion control and performance evaluation of a magnetic-geared dual-rotor motor in hybrid powertrain," *IEEE Trans. Ind. Electron.*, vol. 64, no. 3, pp. 1863-1872, Mar. 2017.

[10] K. D. Hoang, K. Atallah, M. Odavic, J. Birchall, and S. Calverley, "Control development for hybrid vehicle powertrain with magnetic continuously variable transmission," in *Proc. IEEE ESARS-ITEC 2018*, Nottingham, UK, Nov. 7-9, 2018.